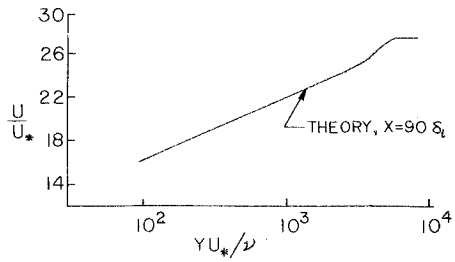

Fig. 3 Mean velocity profile in wall variables.

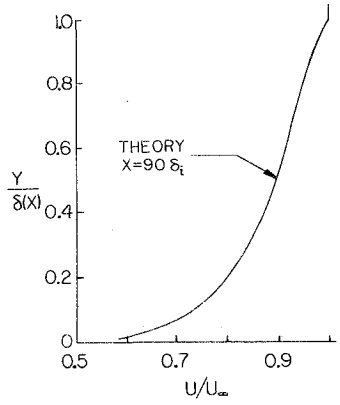

Fig. 4 Mean velocity profile in outer variables.

both variables exhibit a sharp interface or superlayer at $y=\delta(x)$.[3] In Fig. 3, the mean velocity at $x=90\,\delta_t$ is plotted in wall variables. Within the region of validity of the law of the wall, the calculated profile is within 1% of the log profile

$$U/u_* = (1/\kappa)\,\ell n\,(yu_*/\nu) + C$$

where $\kappa=0.41$, $C=5.0$, and u_* is calculated from Eq. (8). The combined law of the wall and wake

$$U/u_* = (1/\kappa)\,\ell n\,(yu_*/\nu) + C + (2\Pi/\kappa)\sin^2(\pi y/2\delta)$$

(where $\Pi=0.62$ for a flat-plate zero pressure gradient turbulent boundary layer[8]) implies a relation between the skin friction and boundary-layer thickness, and therefore the small error in calculating c_f (Fig. 1) precludes comparison with the velocity profile in the wake region. Furthermore, the combined law of the wall and wake, being an unconditional average taken at a fixed distance from the wall, embodies the intermittent structure of the outer region of the boundary layer. The model equations, however, assume no intermittency, and it would therefore be more appropriate to compare the calculated mean velocity as well as the calculated mean turbulence quantities in the outer region with conditional turbulent averages taken at fixed distances from the instantaneous edge of the boundary layer. Such measurements have apparently not been published to date. The mean velocity at $x=90\,\delta_\theta$ is replotted in Fig. 4 in outer variables to display its sharp superlayer at $y=\delta$.

References

[1]Saffman, P. G., "Model Equations for Turbulent Shear Flow," *Studies in Applied Mathematics*, Vol. 53, March 1974, pp. 17-34.

[2]Saffman, P. G. and Wilcox, D. C. "Turbulence-Model Predictions for Turbulent Boundary Layers," *AIAA Journal*, Vol. 12, April 1974, pp. 541-546.

[3]Saffman, P. G., "A Model for Inhomogeneous Turbulent Flow," *Proceedings of the Royal Society (London)*, Vol. A317, 1970, pp. 417-433.

[4]Knight, D. D., "An Analytical Investigation of Turbulent Flow Over a Wavy Boundary," Ph.D. thesis, 1974, Department of Aeronautics, California Institute of Technology, Pasadena, Calif.

[5]Wilcox, D. C. and Alber, I. E., "A Turbulence Model for High Speed Flows," *Proceedings of the 1972 Heat Transfer and Fluid Mechanics Institute*, Stanford Univ. Press, Stanford, Calif. 1972.

[6]Wilcox, D. C., "Calculation of Turbulent Boundary Layer Shock Interaction," *AIAA Journal*, Vol. 11, Nov. 1973, pp. 1592-1594.

[7]Coles, D., "The Young Person's Guide to the Data," *AFOSR-IFP-Stanford Conference on Computation of Turbulent Boundary Layers*, Vol. II,Stanford University Press, Stanford, Calif. 1968.

[8]Keller, H., "A New Difference Scheme for Parabolic Problems," *Numerical Solution of Partial Differential Equations—II*, edited by B. Hubbard, Academic Press, New York, 1970, pp. 327-350.

[9]Klebanoff, P. S., "Characteristics of Turbulence in a Boundary Layer with Zero Pressure Gradient," Rept. 1247, May 1953, NACA.

[10]Hopkins, E. J. and Inouye, M., "An Evaluation of Theories for Predicting Turbulent Skin Friction and Heat Transfer on Flat Plates at Supersonic and Hypersonic Mach Numbers," *AIAA Journal*, Vol. 9, June 1971, pp. 993-1003.

Holographic Analysis of Particle-Induced Hypersonic Bow-Shock Distortions

D.T. Hove* and A.A. Smith†

Science Applications, Inc., El Segundo, Calif.

Introduction

BACKFACE temperature measurements made on thin skin blunt models subjected to dust-laden, hypersonic flows have indicated significantly enhanced stagnation region heating rates over clear air values.[1-3] High-speed shadowgraph movies taken in hypersonic wind tunnels and laser photographs taken in ballistic ranges revealed that the model bow shocks were severely distorted by the particulate in the flow. The bow shock distortions generally had the appearance of large-angle conical shocks which traveled upstream from the bow shock and then collapsed or were swept around the model. Previous investigators[2,3] postulated that the shock distortions were initiated by rebounding dust particles or model ejecta and that the large cone angles were due to communication with the high pressure bow-shock region through the particle wakes.

Tests were performed in the Boeing Hypersonic Wind Tunnel in a Mach 5 combined dust particle/aerodynamic flow environment to investigate the particle-induced bow-shock distortions and their connection with enhanced stagnation region heating rates. As part of the test program, three-dimensional laser holograms were obtained to examine the structure of the bow-shock distortions.

Experiment Description

An in-line laser holocamera mounted perpendicular to the wind tunnel centerline viewed the models through 15-cm optical windows. Coherent light from a 30-millijoule Q-switched ruby laser was used to illuminate the particle field and test model. Duration of the laser pulse was about 15 nsec which effectively froze the particle and shock distortion motion.

The laser power source was charged when the tunnel conditions were being established, and the laser was fired manually about a second after the model reached the tunnel centerline. Holograms were taken of 12 dust tests including two model sizes and materials (2.5 and 6.0 cm titanium and graphite disks), two flow unit Reynolds number (2.8 and

Received October 23, 1974; revision received December 23, 1974. This work was sponsored by the Air Force Space and Missile Systems Organization (SAMSO) under Contract FO4701-73-C-0095.

Index categories: Boundary Layers and Convective Heat Transfer—Turbulent; Shock Waves and Detonations; Supersonic and Hypersonic Flow.

*Staff Scientist. Member AIAA.

†Optical Technician, Tullahoma, Tenn.

6.4×10^5/cm) and two incident particle sizes (100 and 800 μ diam).

Three-dimensional holograms were reconstructed at the SAI Optics Laboratory in Tullahoma, Tenn. The holographic plates were illuminated with a 50-mw helium neon laser, and the scenes were projected onto a ground glass screen for viewing. When a plane containing a particle or shock distortion was brought into focus, the screen was replaced with a Polaroid film pack and photographs taken for permanent record.

Experiment Results

Bow-shock distortions were observed on each of the 12 holograms obtained, and as in the high-speed films, the distortions had the appearance of large-angle conical shocks protruding upstream of the bow shock (Fig. 1). Enlargements of the holograms revealed particles in the apex of some of the shock cones (Fig. 2). The conical shock distortions were not associated with the freestream particle shock structure (the 100-μ particles were traveling subsonic with respect to the flowfield) as illustrated by the fact that for the particular dust loading conditions (0.037 gm/cm^2/sec) of Fig. 1, approximately 50 particles were in the scene volume. Rather, it appeared that some fraction of the particles interacted with the model to produce the bow-shock distortions.

The number of shock distortions on each hologram was approximately a linear function of the particle impingement rate for 100-μ particles independent of model material. A substantially larger percentage of shock distortions occurred for 800-μ flows, but the dependence on impingement rate could not be established from the two 800-μ tests. The longest shock distortions observed on the holograms were 3.2 cm (measured from the body) for 100-μ particle flows, and 4.5 cm for 800-μ particle flows.

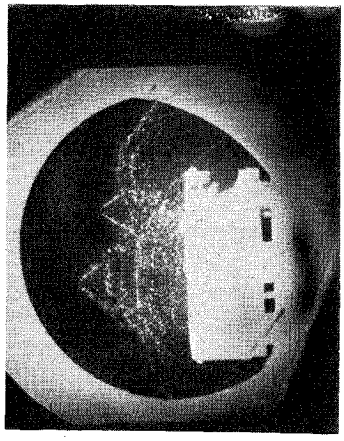

Fig. 1 Bow-shock distortions during 100-μ particulate flow.

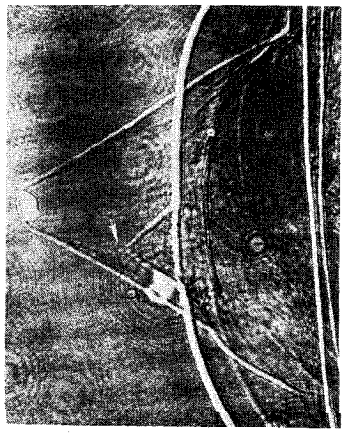

Fig. 2 Bow-shock distortions during 800-μ particulate flow.

Of the 30 well-defined shock distortions examined, 7 clearly had particles in the apex of the shock cone. For 100-μ flows, three shock distortions contained particles which were approximately 100 μ in diameter; for 800-μ particle flows, three shock distortions contained particles with a minimum dimension of 800 μ (Fig. 2) and one shock distortion contained a particle that was less than 100 μ (Fig. 2, arrow). The size of the particles indicated they were primarily rebounded dust particles and not ejecta. All shock distortions for which particles were observed in the apex occurred on tests employing graphite models.

Cone half angles for shock distortions with particles in the apex were consistently less than 40° while the predominant number of shock distortions with no identifiable particle had cone angles greater than 40°. Although no cone angles were as low as the flow Mach angle ($\alpha = 11.5°$), two shock distortions were found with cone angles less than 30°. The two low-cone-angle shock distortions appeared to have escaped from the influence of the bow shock.

Generally, the surfaces of the shock distortions were highly irregular. Enlarged portions of the 100-μ particle flow holograms revealed that the edges of the shock distortions were scalloped whether a particle was present or not. In some cases the apices of cones without identifiable particles did not appear to be closed, although this may have been due to hologram resolution.

The average measured hypersonic bow-shock standoff distance for the 6 cm disks was within 3% of the theoretical result of Serbin.[4] However, the bow-shock standoff distance for the 2.5 cm disks was between 20 and 30% low, apparently due to the dominating effects of large single distortions.

Summary and Conclusions

Three-dimensional laser holography was employed to examine the structure of blunt-body bow-shock distortions in dust-laden, hypersonic flows. As in the high-speed films, the bow-shock distortions appear to be caused by rebounded particles; however, the presence of ejecta in the shock distortions cannot be ruled out. The fact that particles were not observed in the shock distortions for tests employing titanium models is thought to be due to particle breakup (particles smaller than 50 μ could not be resolved). All but two of the shock distortion cone angles were much larger than the flow Mach angle supporting the postulation that communication was maintained between the shock distortions and the high-pressure bow shock region.

A theoretical model based on the Saffman turbulence equations has been used successfully to predict enhanced stagnation point heating rates for low-speed flows.[5] Shock distortions are suspected sources of turbulence and are thought to be connected to the enhanced heating rates. However, the present experimental results show no effect of model material on shock distortion frequency, length or cone angle while enhanced heating rates in particulate environments have been found to correlate with material dependent erosion mass loss rates.[3] Further analytical and experimental investigations are required to model the mechanisms responsible for the enhanced aerodynamic stagnation point heating.

References

[1] Dunbar, L.E. and Courtney, J.F., "Minuteman Hot Structure Heating Augmentation, Study," SAMSO-TR-73-272, Aug. 1973, Space and Missile Systems Organization, Los Angeles, Calif.

[2] Fleener, W.A. and Watson, R.H., "Convective Heating in Dust-Laden Hypersonic Flows," AIAA Paper 73-761, Palm Springs, Calif., 1973.

[3] Dunbar, L.E., Courtney, J.F., and McMillen, L.D., "Heating Augmentation in Particle Erosion Environments," *AIAA Journal*, Vol. 13, Aug. 1975, to be published.

[4]Serbin, H., "Supersonic Flow Around Blunt Bodies," *Journal of the Aeronautical Sciences*, Vol. 25, Jan. 1958, pp. 58-59.
[5]Traci, R.M. and Wilcox, D.C., "Analytical Study of Freestream Turbulence Effects on Stagnation Point Flow and Heat Transfer," this issue, pp. 890-896.

Influence of Probe Geometry on Pitot-Probe Displacement in Supersonic Turbulent Flow

Jerry M. Allen*
NASA Langley Research Center, Hampton, Va.

Nomenclature

D = pitot probe outside diameter
M_e = boundary-layer edge Mach number
R_θ = Reynolds number based on momentum thickness
u = streamwise velocity
u_e = streamwise velocity at boundary-layer edge
y = normal coordinate
α = angle between probe and support shaft (see Fig. 1)
δ = boundary-layer total thickness
θ = boundary-layer momentum thickness
θ_0 = boundary-layer momentum thickness for $D=0$

In a recent *AIAA Journal* Note,[1] Wilson compared the pitot probe interference experiments of Allen[2] with those of Wilson and Young,[3] and concluded that the reason the results of these two experiments did not agree was differences in probe-tip and support geometries. Allen's experiment was conducted with flat-ended probes supported by a shaft of circular cross-section (configuration C of Fig. 1), whereas Wilson and Young's experiment was conducted with beveled probes supported by a thin, diamond-shaped shaft, similar to configuration E of Fig. 1. Both were conducted in turbulent boundary layers on the sidewall of supersonic wind-tunnels.

The probe interference effects obtained in these two experiments are illustrated in Fig. 2 in which velocity profiles measured at similar test conditions are compared. The effects of probe size in Allen's data are much larger than those in Wilson and Young's data; hence the pitot probe displacement effects are correspondingly larger.

In an attempt to analyze these geometric effects, the present author has conducted a further experiment in which the six probe configurations shown in Fig. 1 were tested at the flow conditions of the Ref. 2 experiment. A small flattened probe, used to measure reference profiles, a beveled probe, and a flat-ended probe were tested with both circular- and diamond-shape support shafts so that the effects of probe tip and support geometry could be separated. The objective of this Note is to report the results of these further tests.

The velocity profiles obtained with all six configurations are presented in Fig. 3, which shows that probe support shape had a negligible effect on the measured profiles. Oil-flow photographs of these configurations revealed that the interference region of the circular support shaft, although more extensive than that of the diamond shaft, was nevertheless well downstream of the probe tip. Hence the differences between the results of Refs. 2 and 3 do not appear to be caused by the support shaft. On the other hand, they do not appear to be

Received November 11, 1974.
Index categories: Boundary Layers and Convective Heat Transfer—Research Facilities and Instrumentation.
*Research Scientist, High Speed Aerodynamics Division. Member AIAA.

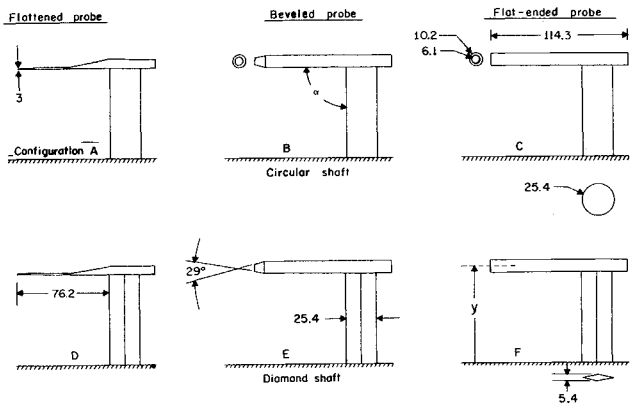

Fig. 1 Probe sketches. (All dimensions in mm.)

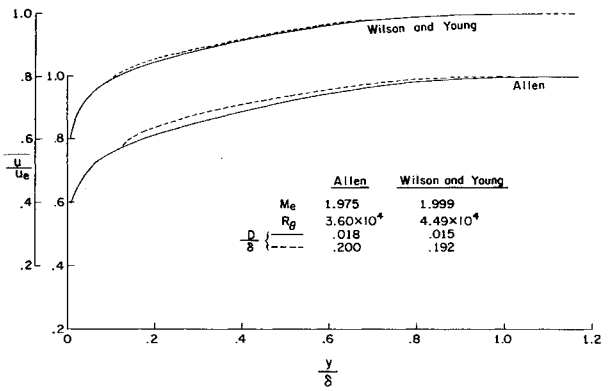

Fig. 2 Comparison of Refs. 2 and 3 probe interference results.

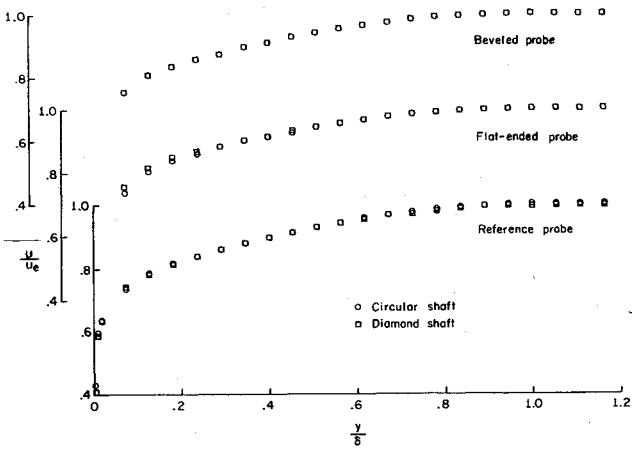

Fig. 3 Effect of support-shaft geometry on measured profiles.

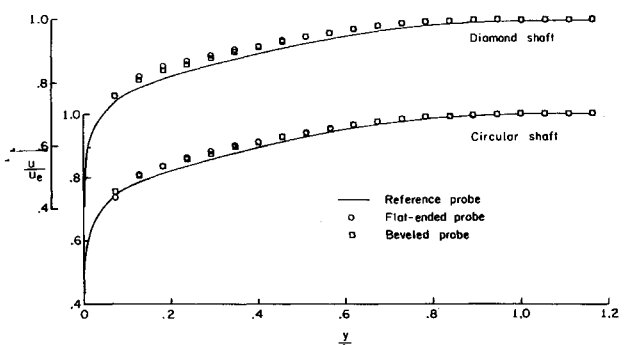

Fig. 4 Effect of probe-tip geometry on measured profiles.